EUROPEAN SYNCHROTRON RADIATION FACILITY
ESRF User Office
BP 220, F-38043 GRENOBLE CEDEX, France
Delivery address: 6 rue Jules Horowitz, 38043 GRENOBLE, France
Tel: +33 (0)4 7688 2552; fax: +33 (0)4 7688 2020; email: useroff@esrf.fr; web: http://www.esrf.fr

Report on Experiment 02 01 800

Insertion of small gold nanoparticules in lyotropic membranes

6 shifts allocated : 15 mars 2010 / 17 mars 2010

B. Pansu

Laboratoire de Physique des Solides , Université Paris-Sud 11, CNRS UMR 8502,

91405 ORSAY Cédex France.

The **aim of the project** was to insert small gold nanoparticules (typically 2nm) inside lyotropic membranes, and in large amount. The dynamics of the membrane was expected to be disturbed and this should be revealed by the shape of the diffraction peaks. Since the nanoparticules are introduced in large amount, we also expected some interaction when confining them inside the membrane, as seen in previously studied systems [1].

1- Materials

Gold nanoparticles have been synthetized using the Brust-Schiffrin method [2] also called two phase-transfer. The gold nanoparticles are formed and stabilized in the organic phase by alkanethiol ligands. Digestive ripening heating the colloidal suspension in the presence of excess of alkanethiol was applied to reduce polydispersity. This technique allows the easy synthesis of monodispersed gold nanoparticles capped by densely packed monolayers, which are air stable. The gold nanoparticles thus prepared can be redispersed in common organic solvents like dodecane without irreversible aggregation or decomposition. Their surface properties can be tailored by changing the grafted ligands and two different ligands have been used: hexanethiol (C6) and dodecanethiol (C12). The diameter of the gold nanoparticles can be finely adjusted by the Au: thiolate ratio and both the temperature and rate at which the reduction is conducted.

Gold nanoparticles have been then redispersed in a mixture of 91 % weight dodecane (Aldrich 99%)and 9% weight pentanol (Sigma Aldrich 99%). Indeed , due to pentanol dissolution in dodecane, a better stability of the lamellar phase is observed when swelled with this mixture, compared to pure dodecane. Samples with various mass fractions of nanoparticles have been prepared: 1%, 5%, 10%, 15%, 20%. For C6-Au (resp. C12-Au) nanoparticles, thermogravimetry analysis has shown that the gold mass fraction was about 88\% (resp. 77%), indicating that about 1/3 of the gold surface sites are bound to a sulphur atom The gold volume fraction in the dodecane+pentanol mixture can thus be estimated to 0.034% (resp.0.03%) for the 1% Au-C6 (resp.Au-C12) nanoparticles mass fraction.

A large amount of lamellar phase without dodecane has been prepared with 30.6% SDS (Fluka 99%), 22% pentanol (Sigma Aldrich 99%) and ultra-pure water (Millipore). Small amounts (about 100 µl) of this primary lamellar phase have been swollen with the different gold dispersions. Below some critical swelling, the dispersions even at low nanoparticles concentration do not penetrate inside the lamellar phase

[1] D. Contantin *et al*, 2008, Repulsion between inorganic particles inserted within surfactant bilayers, *Phys. Rev. Lett.,* 101, 098101.

[2] M. Brust *et al*, 1994, Synthesis of Thiol-derivatised Gold Nanoparticles in a Two-phase Liquid-Liquid, *J. Chem. Soc., Chem. Commun*., 801.

and a phase separation is clearly observed. Above this critical swelling, large amount of gold nanoparticles can easily be incorporated in the lamellar phase and no phase separation is observed during several months or under centrifugation. Three different swellings have been used corresponding to three non doped lamellar phase: 20% (swelling A) , 29% (swelling B), 37% (swelling B) in dodecane mass fraction. These three swellings will be referred next as A, B, C. Following the phase diagram of Safinya and al [3]. These thee different swelling are expected to give an additional hydrophobic layer thickness of about 1.4 nm, 2.7 nm and 3.9 nm. The samples were prepared either in standard X-Ray capillaries (diameter 0.7mm) using smooth centrifugation or in flat glass capillaries (VitroComInc.), 0.1 mm thick and 2 mm wide by gently sucking in the lamellar phase using a syringe. The capillaries were then sealed.

2- Configuration of the line: The small angle x-ray scattering measurements were performed on the bending magnet line BM02 5D2AM) at a photon energy of 10.7 keV. The data were acquired using a CCD peltier cooled camera (SCX90-1300, Princeton Instruments Inc.) with a resolution of 1340x1300 pixels. Data preprocessing (dark current substraction, flat field correction, radial regrouping and normalization) was performed using the software developed at the beam line. The accessible scattering range was $0.02<q<0.48$ Å^{-1} (distance sample to detector : about 38 cm). Some kapton windows have been replaced by mica sheets. Beam stop=2.5 mm diameter.

3- Particles and initial dispersions

a) The size of the gold core has been measured again on diluted dispersion of gold nanoparticles in dodecane: radius R= 1.20 nm with 15% polydispersity for C6-Au and R=1.05 nm with 10%polydispersity for C12-Au). The UV-visible absorbtion spectra performed on very dilute solutions (0.1\% weight) are compatible with these values.

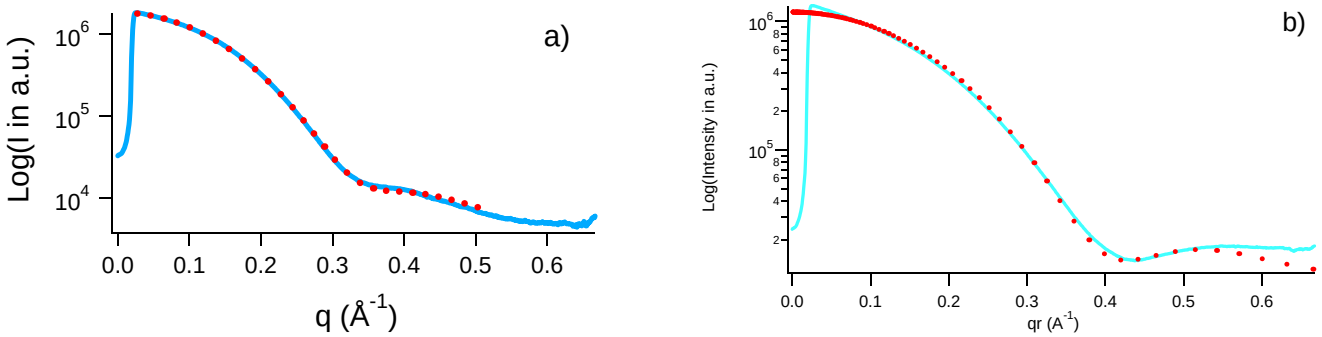

Figure 1: Form factor of Au-C6 (a) and Au-C12 (b) nanoparticles
Experimental form factor: in blue , Polydisperse sphere form factor in red

b) The intensity scattered by the various dispersions in dodecane has been measured. For the lowest concentration (1% mass), the intensity profile is well described by the form factor of a sphere F(qR) with a radius R that corresponds only to the gold core size since there is no X-ray contrast between the capping agent and the solvent. At higher concentrations (above 5% weight dispersions), the interaction between the particles is visible since the structure factor defined as $S(q)=I(q)/F(qR)^2$ is no longer equal to 1. Fig. 2 shows the structure factor for the different dispersions.

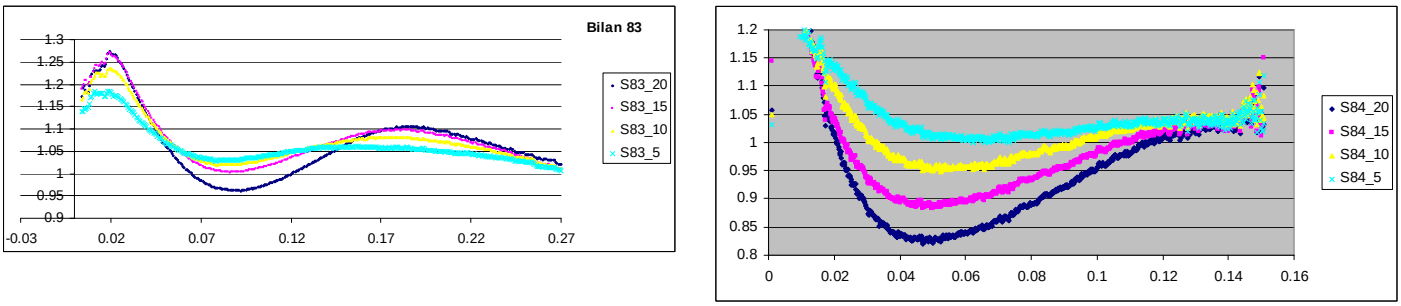

[3] C.R. Safinya *et al*, 1986, Steric Interactions in a Model membrane System : a Synchrotron X-Ray Study, *Phys.Rev.Lett* ,**57**, 2718

Fig 2a: Structure factor of the Au-C6 dispersions
Left axis: S(q) Bottom axis: q in $Å^{-1}$

Fig 2a: Structure factor of the Au-C12 dispersions
Left axis: S(q) Bottom axis: q in $Å^{-1}$

Interactions between particles have clearly a repulsive part attributed to the repulsion between the thiol capping agents and an attractive part that can be seen at short q attributed to Van der Waals interaction between the gold cores. Theoretical approach has been performed in order to determine the apparent radius of the nanoparticles (gold+ thiol capping). Repulsion has been treated as hard sphere repulsion with an apparent radius R using Percus-Yevick approach. Van der Waals attraction has been treated through the RPA approximation using a Hamaker constant A=75kT. The only variable parameter in these curves is the nanoparticles apparent radius which has been adjusted using the maximum position of S(q). For Au-C12 (resp. Au-C6) gold nanoparticles, this radius is 2.2 nm (resp 1.6 nm). The paraffinic chain thickness is as expected larger for C12 chain than for the C6 chains. The difference between experimental and theoretical structure factor is probably due to the fact that treating the steric repulsion as hard sphere is certainly too crude and that the RPA approximation may be not valid.

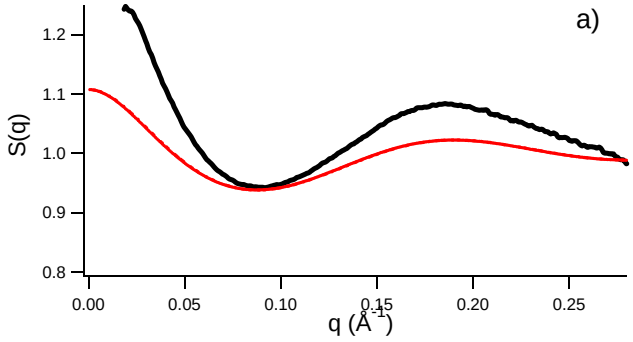

Fig 3a: Structure factor of the 20% Au-C6 dispersion (in black) compared to theoretical structure factor (in red)

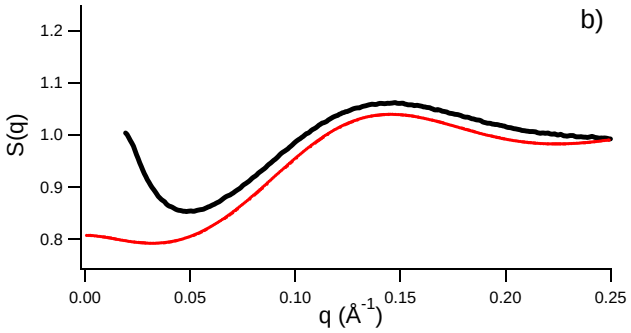

Fig 3a: Structure factor of the 20% Au-C12 dispersion (in black) compared to theoretical structure factor (in red)

4) Doped lamellar phases

Diffraction patterns performed on lamellar phases containing gold nanoparticles have revealed that most samples prepared with the Au-C6 dispersions are quite well oriented, mainly with planar alignment as shown in Fig.4 even in the cylindrical capillaries. Only few samples prepared with the Au-C12 dispersions were perfectly oriented. This could be due either to the larger size of the particles that disturb more the structure or just that the samples had been prepared not enough in advance.

Figure 4: Diffraction patterns obtained on oriented samples (Au-C6)

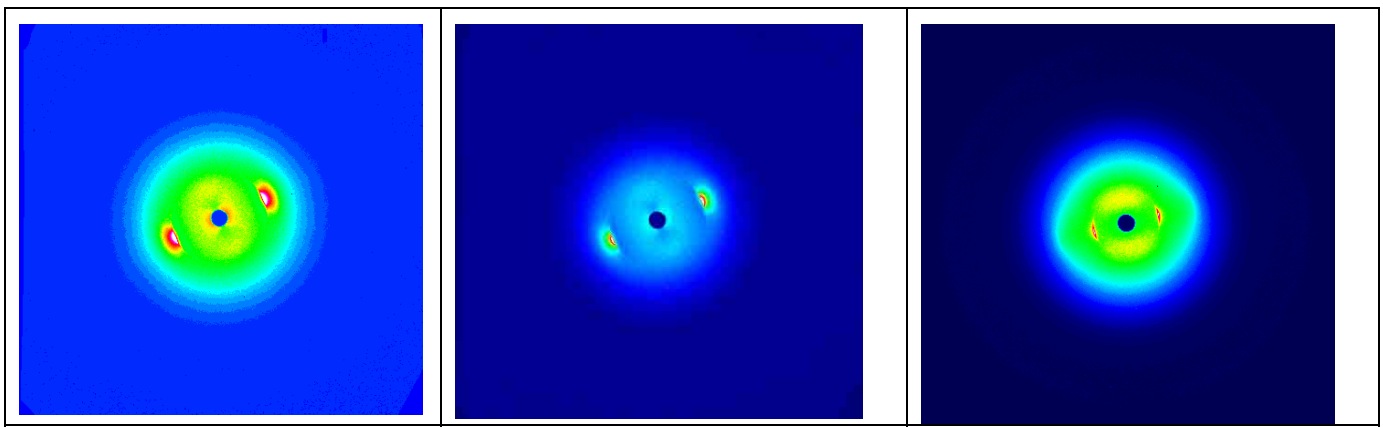

Au-C6, 20%, swelling rate A	Au-C6, 20%, swelling rate B	Au-C6, 20%, swelling rate C

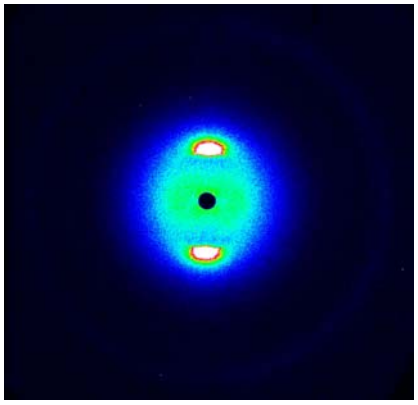	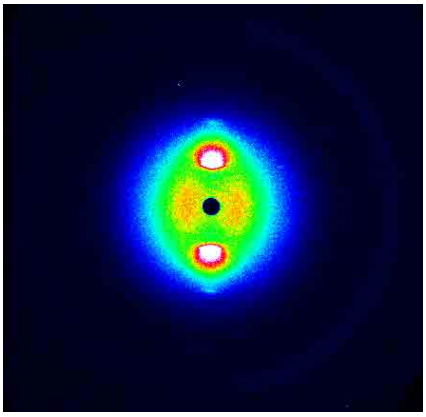	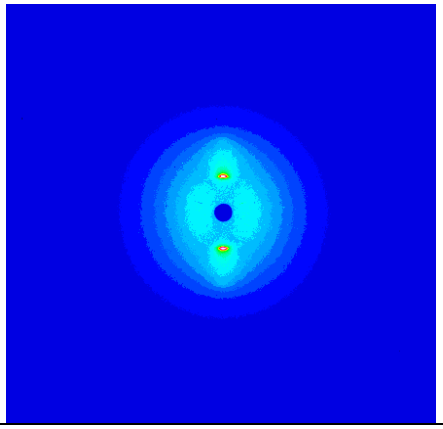
Au-C6, 15%, swelling rate A	Au-C6, 15%, swelling rate B	Au-C6, 15%, swelling rate C
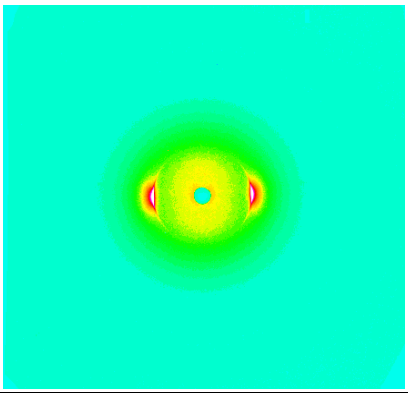	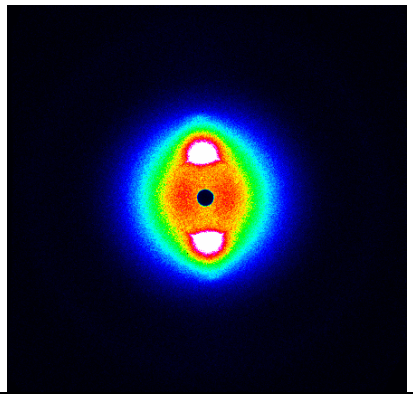	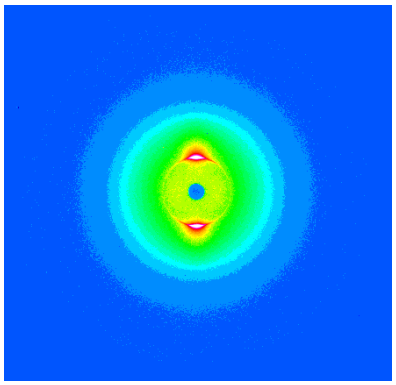
Au-C6, 10%, swelling rate A	Au-C6, 10%, swelling rate B	Au-C6, 10%, swelling rate C
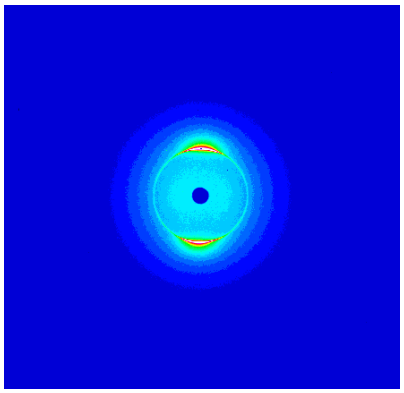	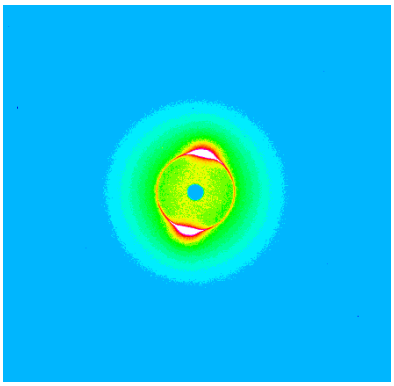	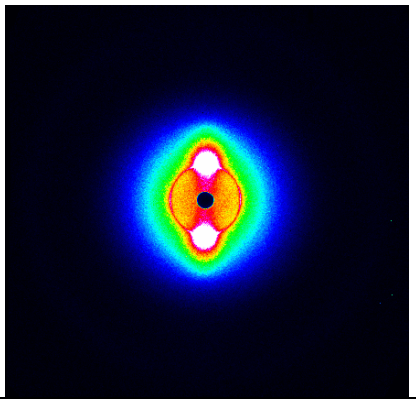
Au-C6, 5%, swelling rate A	Au-C6, 5%, swelling rate B	Au-C6, 5%, swelling rate C
	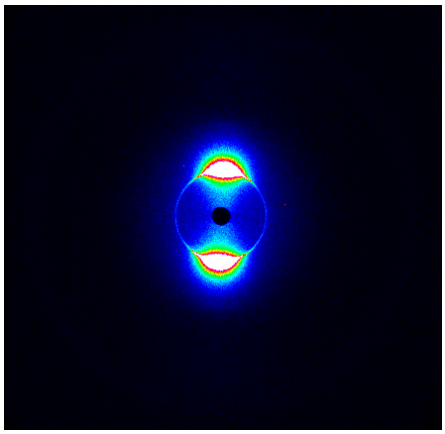	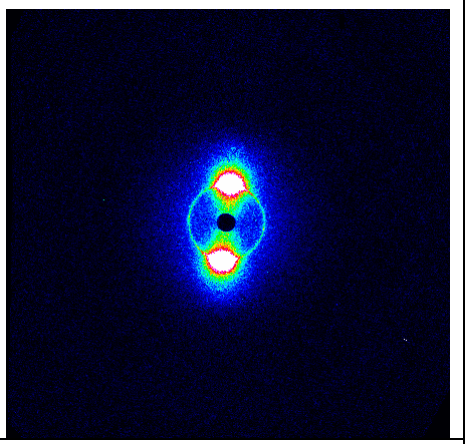
	Au-C6, 1%, swelling rate B	Au-C6, 1%, swelling rate C

The strong Bragg reflection indicates the direction of the lamellar periodicity (refered as the z direction). Only first order is clearly identified and its position is a direct measurement of the lamellar spacing: 5.26 nm for swelling A, 6.39 nm for swelling B, 7.84 nm for swelling C in good agreement with the phase diagram of Safinya *et al*.

Interaction between particles

In these patterns, the contribution of the gold nanoparticles is clearly anisotropic, mainly for swelling B and C. It is more intense in the x direction (perpendicular to the z direction) than in the z direction. This confirms that the nanoparticles are confined in the hydrophobic part of the lamellar phases and are thus periodically distributed along the z direction. The interesting feature is that the scattering diffusion along the x direction exhibits some maximum at a finite q value. We have mesaured the scattered intensity inthe x direction along a line. Taking into account the nanoparticles form factor reveals that the structure factor of the nanoparticles $S_x(q_x)$ in the lamellar plane is very different from that of pure dispersions.

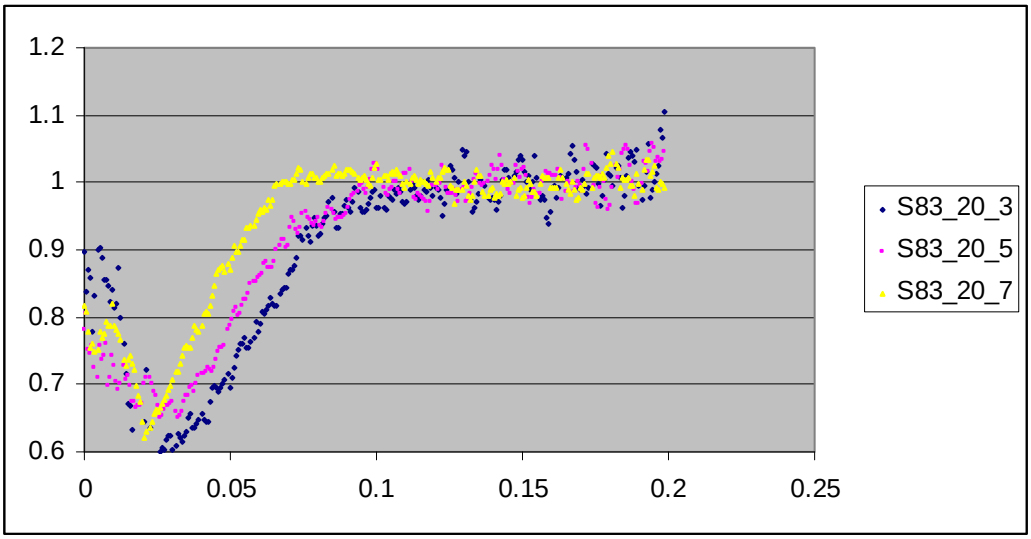

Figure 5: $S(q_x)$ for different samples containig 20% Au-C6 dispersions at different swelling

A: blue B: pink, C: yellow

There is clearly additional repulsive interaction induces by the confinement in the lamellar phase. The repulsive pair potential can be estimated from $S_x(q_x)$ using a RPA approximation:

$$\frac{n\widetilde{U}(q_x)}{k_B T} \approx \frac{1}{S(q_x)} - 1$$

where n is the particle surface density . The pair potentiel U(r) between particles in the layer has been approximated using a Gaussian function:

$$U(r) = U_0 \exp - \left(\frac{r^2}{2\xi^2} \right).$$

Its Fourier transform in 2D is then simply given by $\widetilde{U}(q) = 2\pi\xi^2 U_0 \exp - \left(\frac{q^2\xi^2}{2} \right)$.

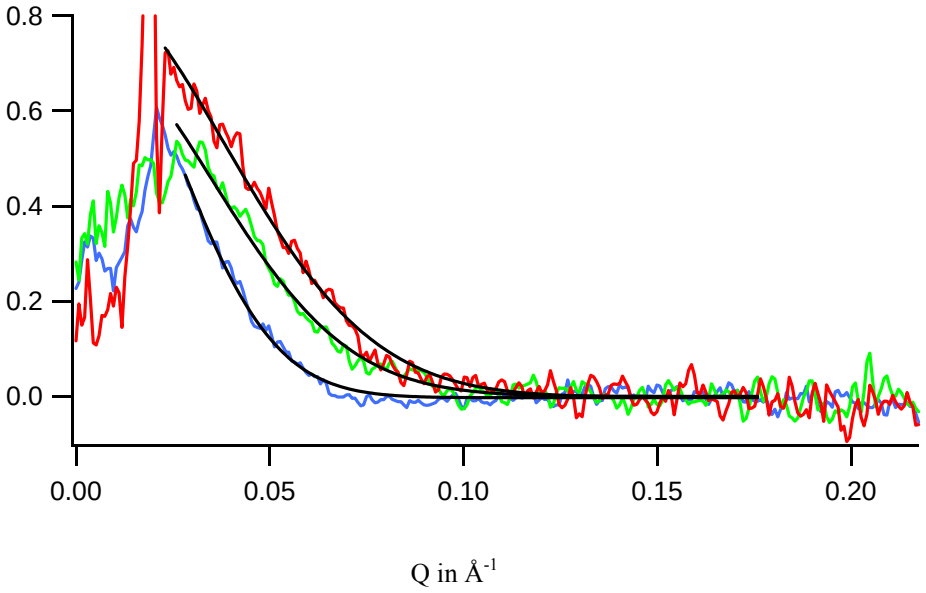

Figure 5: Determination of the repulsive potential $n\tilde{U}(q_x)$ between the particles for solution 20% weight in Au-C6 Effect of swelling : in blue (C) , in green (B), in red (A)

Some values of ξ and U_0 ae given in the following table

Sample	Lamellar period (in nm)	Additional thickness in nm	Particle surface density (nm^{-2})	Apparent surface disk fraction	Mean distance between particles (in nm)	ξ in nm Error ≈ 20%	U_0/k_BT Error ≈ 20%
Au-C6 20% A	5.3	1.4	0.0013	0.01	28	2.6	16
Au-C6 20% B	6.4	2.7	0.0024	0.02	20	2.9	6
Au-C6 20% C	7.85	3.9	0.0035	0.053	17	3.9	3
Au-C6 10% B	6.4	2.7	0.0012	0.01	29	3.5	5
Au-C12 10% B	6.4	2.7	0.0016	0.025	25	2.7	11

The additional repulsion induced by the confinement of nanoparticles in the hydrophobic part is quite large in intensity and in range and competes seriously with Van der Waals interaction. It cannot be attributed to electrostatic interaction between the inserted objects as already seen for transmembrane proteins. The intensity of the confinement-induced repulsive potential increases with decreasing swelling rate. It also depends on the global size of the particles and increases with the capping agent length. The lateral range of this interaction clearly depends on the swelling rate and is roughly proportional to the lamellar period. Complementary experiments are needed to precise the influence of the particle size on the lateral range. On this purpose homeotropic alignment would help in improving experimental resolution of $S(q_x)$ Nevertheless it is clear that confinement has a great influence on the particle interaction. The global particle size 3.2 nm diameter for C6-Au and 4.4 nm diameter for C12-Au is of the same order of magnitude as the additional thickness induces by swelling but either larger or smaller (A:1.4 nm , B: 2.7 nm and C:3.9 nm). In the case of the smallest swelling (A), it is clear that the layers are strongly disturbed by the particles and that this can induce additional repulsion as for inorganic clusters in lipid membranes. Nevertheless one can also wonder whether particles are really located inside the hydrophobic layers or create defects like bridges between the layers. Moreover this is probably not the only mechanism since additional repulsion is also observed when the particles are smaller than the swelling thickness. One possible explanation is that the presence of the particles acts on fluctuation modes of the different layers and that two particles approaching each other will kill some fluctuations modes. The range of the

interaction would be given by the largest allowed wavelength ξ_0 at energy k_BT which is known to be proportional to the smectic period : $\xi_0 \approx d\sqrt{\frac{\kappa}{k_BT}}$ where κ is the curvature modulus of a surfactant layer.

Effects on layers fluctuations

The presence of the inclusions inside the membrane was suspected to modify its flexibility and this was expected to be seen in the change of the lamellar peaks profile (algebric decay). The influence of swelling on the lamellar peak profile has been largely studied by Safinya *et al* and is well know for this system. Different models[4] have been proposed to analyse the peak profile, driven by the same parameter defined in terms of the elastic constants of the smectic phase: $\eta = \frac{\pi k_B T}{2d^2\sqrt{K\bar{B}}}$. No significant change in the peak profile has been detected as no real increase of the second order peak.

The main change around the peak is the increase of an anisotropic diffusion when adding particles that extends at larger q_z. More particles are added more anisotropy is observed. At present we do not understand the origin of this strong and anisotropic diffusion around the smectic peak.

At low q, diffuse scattering is also observed along the z direction at smaller swelling but whatever the particle concentration is. This is certainly linked to defects of the lamellar structure.

Conclusion

Two main results were expected: the interaction between the gold nanoparticles especially at high concentration and the effect of the inclusions on the membrane flexibility.

1) Scattering on planar orientad samples reveals unambuiguously the contribution of the lamellar structure and of the particles. Additive repulsive interaction between the particles have clearly been seen (paper in preparation). But more precise determination of the interaction potential requires homeotropic alignment, that is not easy to obtain with this ionic system that does not "melt" a higher temperature.

   Increasing the particle concentration also worth to be done. One expect that above some critical concentration particles will be expelled from the layer but local order could be seen before.

2) Unfortunately no significative change in the smectic profile could be detected. Adding particules change the diffusion around the peak which becomes strongly anisotropic in the smectic order direction. No simple interpretation of this anisotropic diffusion can yet be proposed.

[4] F. Nallet *et al*, 1993, Modelling X-Ray or neutron scattering spectra of lyotropic lamellar phases : interplay between form and structure factors, *J. Phys. II France* , 3, 487-502